# Electronic Supplementary Information (ESI)†
# The Structural Complexity of Perovskites

Sebastian Hallweger,[a] Clemens Kaußler,[a] and Gregor Kieslich*[a]

[a] *Technical University of Munich, Department of Chemistry, Lichtenbergstraße 4, Garching, GER;*
*E-mail: Gregor.Kieslich@tum.de*

## Contents

# 1 Methodological Remarks

## 1.1 Comparison of Complexity Measures

### 1.1.1 Combinatorial vs Configurational Complexity

In recent publications,[1,2] combinatorial ($I_\mathrm{G}$ here referred to as $I_\mathrm{G,comb}$) as well as configurational information contents ($I_\mathrm{G,conf}$) have been used in order to compare structural complexity. Both measures are given in the full dataset (section 2). Owing to a higher discriminatory character of the configurational complexity values that improves on the differentiation between the complexity of crystal structures, we have decided to largely discuss $I_\mathrm{G,conf}$ in the main paper. However, similar trends are obtained for combinatorial complexities (also see supplementary plots in subsection 1.2).

For details on the differences between both complexity measures, we want to refer to the paper by W. Hornfeck[2], and here we only provide a few examples of how the calculation of $I_\mathrm{G,conf}$ provides additional opportunities in the differentiation of crystal structure complexities. For instance looking at examples in the family of inorganic perovskites, where $BaTiO_3$, $KNbO_3$ and $BiFeO_3$ have identical combinatorial complexity values $I_\mathrm{G,comb}$ of $1.371\,\frac{\mathrm{bit}}{\mathrm{position}}$, but differ in their coordinational complexity values $I_\mathrm{G,coor}$ with $1.500\,\frac{\mathrm{bit}}{\mathrm{arity}}$ for $BaTiO_3$ and $KNbO_3$ and $1.371\,\frac{\mathrm{bit}}{\mathrm{arity}}$ in the case of $BiFeO_3$. The calculation of $I_\mathrm{G,conf}$ of these structures results in $2.419\,\frac{\mathrm{bit}}{\mathrm{pos.\ \&\ arity}}$ for $BaTiO_3$ and $KNbO_3$ and $2.289\,\frac{\mathrm{bit}}{\mathrm{pos.\ \&\ arity}}$ for $BiFeO_3$.

Interestingly, equal values of combinatorial complexities can also be found in the comparison of different perovskite families. The thiocyanate-bridged compound $Cs[Cd(SCN)_3]$ and the hybrid perovskite $(PIP)[NaI_3]$ show the same combinatorial complexity value $I_\mathrm{G,comb}$ of $3.550\,\frac{\mathrm{bit}}{\mathrm{position}}$. Because of different coordinational complexities between the two structures ($3.322\,\frac{\mathrm{bit}}{\mathrm{arity}}$ for $Cs[Cd(SCN)_3]$ and $3.420\,\frac{\mathrm{bit}}{\mathrm{arity}}$ for $(PIP)[NaI_3]$), configurational complexities become distinguishable: $4.432\,\frac{\mathrm{bit}}{\mathrm{pos.\ \&\ arity}}$ for the thiocyanate structure and $4.475\,\frac{\mathrm{bit}}{\mathrm{pos.\ \&\ arity}}$ in case of the HOIP.

These examples demonstrate that not only the inclusion of arities into the calculation, but the mathematical approach itself with a strong additive sum instead of a simple addition, achieves a higher discriminating character in the analysis of the configurational complexities. Therefore, the configurational entropy $I_\mathrm{G,conf}$ is a suitable value for the comparison of the evaluated perovskite structures.

### 1.1.2 Advantage of Information Theory over Number of Atoms in Reduced Unit Cell $\nu$

It has repeatedly been suggested to simplify complexity calculation to the number of atoms in the reduced unit cell or closely related measures,[3–5] $\nu$, as it seems a suitable parameter for complexity comparison at first. But not only is this approach limited with regards to comparisons across different material classes, it also oversimplifies the intricacies of crystal structures to a degree that the obtained complexity parameter does not reflect chemical intuition well. On the one hand, this means that the overall complexity order which one might assign to a series of compounds by gut feeling does not correspond to the calculated complexity values. This shortcoming of $\nu$ has already been demonstrated vividly by S. Krivovichev by comparison of sodium chloride, rutile, and barium titanate.[5] On the other hand, many well-distinguishable crystal structures have an equal number of atoms in their reduced unit cell, erroneously resulting in equal complexities. Not only is the logarithmic scale of information theoretical measures a better reflection of human complexity assessment, it further aids comparability, as the linear character of $\nu$ causes the parameter to reach large magnitudes which often erroneously suggest pronounced complexity differences that do not conform with intuition. In contrast, $I_\mathrm{G,comb}$ does not usually exceed values of $11\,\mathrm{bit\,pos.}^{-1}$.[2] Furthermore, categorizing atoms according to their crystallographic orbits leads to the consideration of symmetry, thereby adding a level of information which is intuitively recognized but left out in case of $\nu$. Finally, it shall be noted that the number of atoms in reduced unit cells of solid solutions is invariant with respect to their composition, whereas a correlation between composition and complexity exists, as evident from entropical considerations. The relationship between $B$-$B$ distance and $\nu$ for our perovskite dataset is shown in Figure S2, with the absence of a clear correlation between the two parameters.

## 1.2 Supplementary Complexity Plots

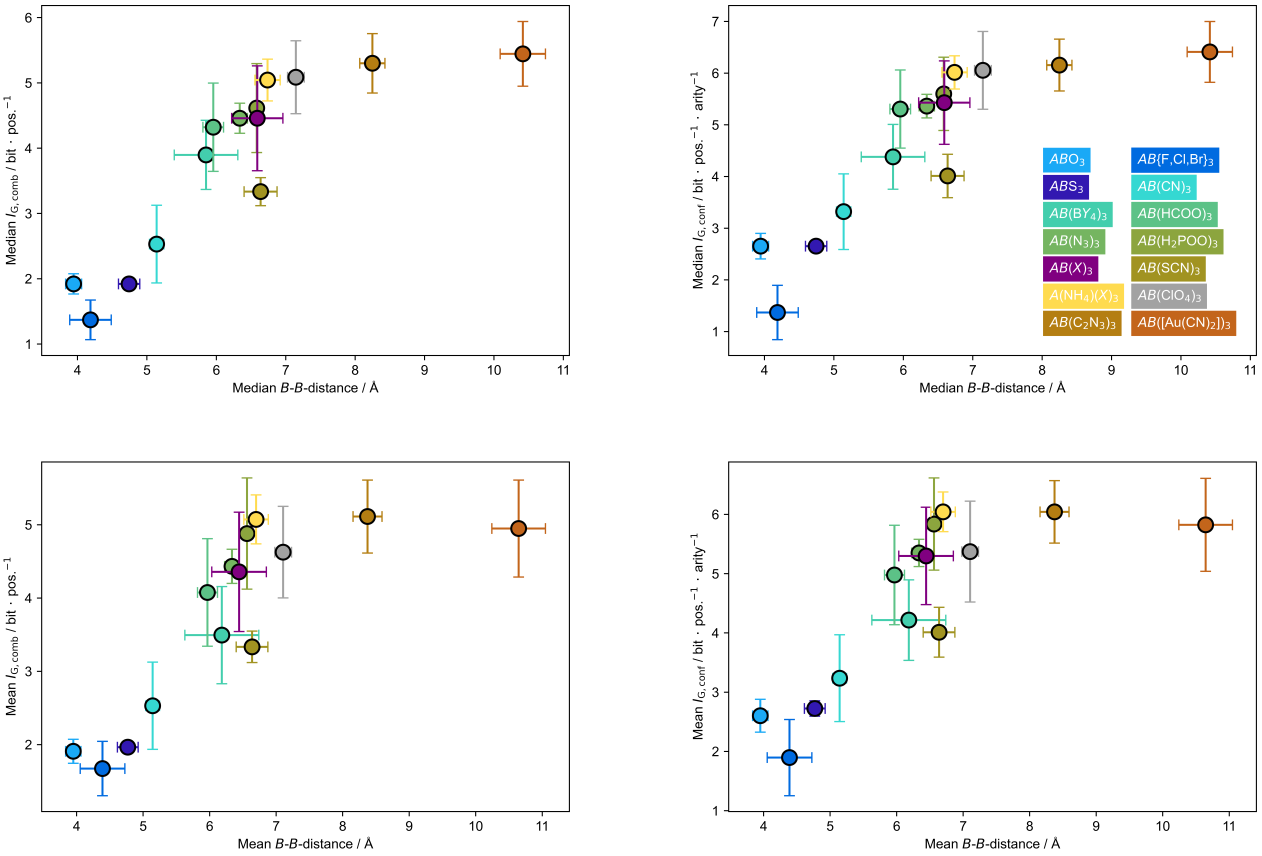

**Figure S1:** Top: median plots, deviation as mean absolute deviation around the median. Bottom: mean plots, deviation as mean absolute deviation around the mean. Left: $I_{\mathrm{G,comb}}$. Right: $I_{\mathrm{G,conf}}$. The same overall complexity trends are observed for combinatorial $I_{\mathrm{G}}$ ($I_{\mathrm{G,comb}}$) and configurational $I_{\mathrm{G,conf}}$ values. Outliers, which are given greater weight in mean compared to median plots, distort trends in former cases. This effect is well-reflected by larger y-error bars in mean plots. Thus, median values are better suited for trend evaluation in this dataset.

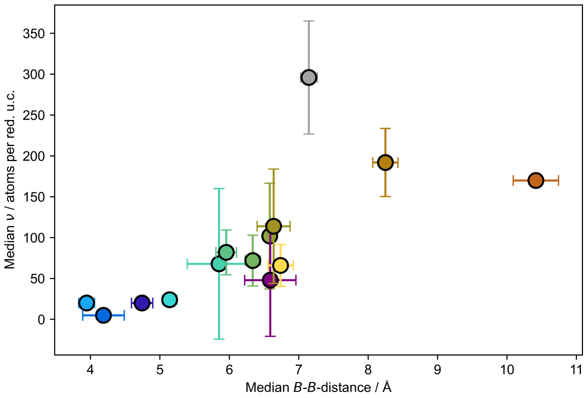

**Figure S2:** Relationship between $B$-$B$ distance and number of atoms in the reduced unit cell, $\nu$. In comparison with complexity parameters that are derived from information theory (see Figure S1), there is only a weak correlation to the $B$-$B$ separation.

## 1.3 Artifacts in Complexity Calculations

In order to obtain meaningful complexity trends, it is pivotal to compile a dataset with carefully selected structures. Some of the criteria for crystal structure selection, which have been presented in the main text, are elaborated on in the following sections.

### 1.3.1 Disordered Molecular Fragments and Co-Crystallized Solvent

An extreme case of molecular disorder can be found in the high-temperature, cubic structure of $MAPbI_3$, in which the *A*-site methylammonium cation is 26-fold disordered, with additional rotational disorder of its methyl groups.[6] The complexity of its published structure (unmodified *.cif file) would amount to $I_{\mathrm{G,comb}} = 4.185\,\mathrm{bit\,pos.}^{-1}$, despite far too low reported occupancies (sum formula $(C_{0.2154}H_{5.4612}N_{0.2154})[PbI_3]$). Its actual information content would thus be even higher. In comparison, methylammonium lead iodide's low-temperature, ordered phase (*Pnma*), as reported in Table S8, has a considerably lower complexity of $I_{\mathrm{G,comb}} = 3.085\,\mathrm{bit\,pos.}^{-1}$. We argue, that for such extreme cases of positional disorder, *.cif files are not suitable anymore to accurately portray the molecular situation. As a result, we do not consider crystal structures with disordered molecular fragments.

Furthermore, crystal structures with solvent molecules are also disregarded. Not only are solvent molecules often highly disordered, but they are also irrelevant to the actual perovskite structure and should be treated separately for complexity calculations. Therefore, only crystal structures without co-crystallized solvent have been chosen for the database.

### 1.3.2 Solid Solutions and Polymorphism

Solid solutions have been excluded from the dataset because of their continuous nature which would either require to chose a representative example of the solution or make comparison between mean or median values necessary. If instead all reported members of solid solutions were to be included in the dataset, these would have a disproportionally high impact on the complexity calculations. Therefore, only chemically distinct compounds without fractional occupation of crystallographic sites were included.

This is also related to the existence of different phases of the same compound, for example at different temperatures or pressures. Only the thermodynamic, ambient pressure phase is chosen in case of multiple known polymorphs of the same compound. Case studies are obviously exempt from this rule.

### 1.3.3 Unresolved Hydrogen Atoms

Many crystal structures, especially older ones, are reported without hydrogen atoms, despite undisputed presence of hydrogen in the material. This is related to weak scattering properties of hydrogen that impede with their crystallographic localization (low electron count resulting in low atomic form factor), especially in the presence of heavy elements. In many cases, hydrogen positions are calculated into the partially solved crystal structure, which is compatible with information theoretical information content determination, provided that the calculation leads to correct Wyckoff positions. However, missing information on the position of hydrogen results in an underestimation of the crystal structure's information content. This is exemplarily demonstrated for $KCd(HCOO)_3$, which has been reported without resolved hydrogen positions for the formate linkers.[7] In comparison with its structurally equivalent but H-resolved manganese congener, $KMn(HCOO)_3$,[8] it becomes obvious that the hydrogen positions contribute to a structure's complexity (*cf.* Table S1). Therefore, crystal structures which are missing hydrogen positions were not included in the dataset.

**Table S1:** Effect of missing hydrogen positions on crystal structure complexity. Unresolved atomic positions are marked with curly brackets.

| Compound | Space Group | $I_{\mathrm{G,comb}}$ [bit pos$^{-1}$] | $I_{\mathrm{G,conf}}$ [bit pos$^{-1}$ arity$^{-1}$] |
|---|---|---|---|
| $KCd(\{H\}COO)_3$ | *C*2/*c* (15) | 2.732 | 3.586 |
| $KMn(HCOO)_3$ | *C*2/*c* (15) | 3.093 | 3.963 |

### 1.3.4 (Partially) Deuterated Structures

Contrary to missing information of hydrogen atoms, partial deuteration of a compound can increase its information content, if deuteration causes Wyckoff positions to be split compared to their protium analog structure. However, none such examples were encountered. Fully deuterated species such as $[CD_3ND_3][GeCl_3]$[9] feature the same information content as their proton equivalent structure and are included in the database. If (partially) deuterated crystal structures coexist with the fully protonated analog of identical structure and complexity, only one of the available structures is included in the dataset. For example, the low-temperature phases of $[CD_3ND_3][PbI_3]$, $[CD_3NH_3][PbI_3]$, and $[CH_3ND_3][PbI_3]$[10] are equally complex as $[CH_3NH_3][PbI_3]$.[11] Only the latter structure was incorporated in the database in order to prevent the compound from being over-represented. The same principle would hold for otherwise isotopically labelled structures, but no examples appeared during data collection.

## 1.4 Modification of Ambiguous Crystallographic Information Files

Some of the crystallographic information files (CIFs) included crystallographic ambiguities, which would have led to erroneous computational results. All adjusted compounds have been marked with an asterisk (*) in the tables below (section 2). Details on the modifications are explained in the following paragraph.

All four TeMA-accommodating compounds of the azido family contained three duplicated hydrogen atoms at one of their methyl groups, with an assigned occupancy of 0.5 but identical coordinates. Duplicates have been deleted from these structures and occupancies at the remaining positions have consequently been adjusted to 1. The crystallographic information file of $(AZ)[Cu(HCOO)_3]$ included atypical occupancy values between 0.86 and 1 for nearly all listed Wyckoff positions. The origin of these reduced occupancies remained unclear since occupancy values of atoms even varied within a substituent (e.g. formate groups with different values for the two oxygen values as well as for hydrogen and carbon). There was no information on occupancy values given by the authors, neither in the main text nor in the Supporting Information of the original publication. The affected positions were therefore adjusted to occupancies of 1. In the original file of $(Gua)[Mn(H_2POO)_3]$, the hydrogen atoms of the hypophosphites and of one of the guanidinium $NH_2$-groups included duplicates with split occupancies, which have been deleted and the occupancy values have been corrected. Lastly, the $(MHy)[Mn(H_2POO)_3]$ file contained duplicates with split occupancies for hydrogen atoms of the central $NH_2$ group and the methyl group of the methylhydrazinium cations. The file was corrected by deletion of duplicates and adjustment of remaining occupancies, in analogy to ambiguous TeMA azides.

## 1.5 Computation of $B$-$B$ distances

The distance between neighboring $B$-cations is reported as average of the center-to-center distances to the six closest $B$-site cations. For example for ammonium cations in metal-free perovskites, the coordinates of their central nitrogen atom was used for measurements, as it marks the molecular cation's center of gravity. Lengths were measured based on the original *.cif files in VESTA. In case of crystallographically inequivalent $B$-sites, their $B$-$B$ distances were averaged again. If a chosen publication includes multiple crystal structures of the same phase, distances are based on the structure which has been recorded at the lowest temperature and pressure.

# 2 Perovskite Data Set

**Table S2:** Space groups and references for inorganic perovskite compounds.

**Ia Oxide-bridged inorganic perovskites**

| Compound | Space Group | ø B-B Dist. [Å] | A-Site Atom Count | $I_{\mathrm{G,comb}}$ [bit pos.$^{-1}$] | $I_{\mathrm{G,conf}}$ [bit pos.$^{-1}$ arity$^{-1}$] | Ref. |
|---|---|---|---|---|---|---|
| $\mathrm{BaTiO_3}$ | $R3m$ (160) | 4.004 | 1 | 1.371 | 2.419 | 12 |
| $\mathrm{CaTiO_3}$ | $Pnma$ (62) | 3.822 | 1 | 1.922 | 2.653 | 13 |
| $\mathrm{PbTiO_3}$ | $P4mm$ (99) | 3.987 | 1 | 1.922 | 2.948 | 14 |
| $\mathrm{PbVO_3}$ | $P4mm$ (99) | 4.085 | 1 | 1.922 | 2.948 | 15 |
| $\mathrm{KNbO_3}$ | $R3m$ (160) | 4.016 | 1 | 1.371 | 2.419 | 16 |
| $\mathrm{SrTiO_3}$ | $I4/mcm$ (140) | 3.248 | 1 | 1.922 | 2.187 | 17 |
| $\mathrm{BiFeO_3}$ | $R3c$ (161) | 3.965 | 1 | 1.371 | 2.289 | 18 |
| $\mathrm{LaYbO_3}$ | $Pna2_1$ (33) | 4.185 | 1 | 2.322 | 3.307 | 19 |
| $\mathrm{YAlO_3}$ | $Pnma$ (62) | 3.706 | 1 | 1.922 | 2.653 | 20 |
| $\mathrm{BaTbO_3}$ | $Imma$ (74) | 4.277 | 1 | 1.922 | 2.624 | 21 |
| $\mathrm{CdTiO_3}$ | $Pna2_1$ (33) | 3.828 | 1 | 2.322 | 3.307 | 22 |
| $\mathrm{DyScO_3}$ | $Pbnm$ (62) | 3.954 | 1 | 1.922 | 2.653 | 23 |
| $\mathrm{EuRhO_3}$ | $Pbnm$ (62) | 3.888 | 1 | 1.922 | 2.653 | 24 |
| $\mathrm{EuScO_3}$ | $Pbnm$ (62) | 3.978 | 1 | 1.922 | 2.653 | 25 |
| $\mathrm{GdFeO_3}$ | $Pnma$ (62) | 3.862 | 1 | 1.922 | 2.653 | 26 |
| $\mathrm{GdScO_3}$ | $Pnma$ (62) | 3.967 | 1 | 1.922 | 2.653 | 27 |
| $\mathrm{HoScO_3}$ | $Pbnm$ (62) | 3.944 | 1 | 1.922 | 2.653 | 23 |
| $\mathrm{LaAlO_3}$ | $R\bar{3}c$ (167) | 3.786 | 1 | 1.922 | 1.686 | 28 |
| $\mathrm{LaCoO_3}$ | $C2/c$ (15) | 3.816 | 1 | 1.922 | 2.657 | 29 |
| $\mathrm{LaCrO_3}$ | $Pnma$ (62) | 3.883 | 1 | 1.922 | 2.653 | 30 |
| $\mathrm{LaCuO_3}$ | $R\bar{3}c$ (167) | 3.864 | 1 | 1.371 | 1.686 | 31 |
| $\mathrm{LaErO_3}$ | $Pnam$ (62) | 4.218 | 1 | 1.922 | 2.653 | 32 |
| $\mathrm{LaFeO_3}$ | $Pnma$ (62) | 3.925 | 1 | 1.922 | 2.653 | 33 |
| $\mathrm{LaGaO_3}$ | $Pnma$ (62) | 3.891 | 1 | 1.922 | 2.653 | 34 |
| $\mathrm{LaInO_3}$ | $Pnma$ (62) | 4.119 | 1 | 1.922 | 2.653 | 35 |
| $\mathrm{LaMnO_3}$ | $Pnma$ (62) | 3.942 | 1 | 1.922 | 2.653 | 36 |
| $\mathrm{LaNiO_3}$ | $R\bar{3}c$ (167) | 3.832 | 1 | 1.371 | 1.686 | 37 |
| $\mathrm{LaPdO_3}$ | $Pnma$ (62) | 4.008 | 1 | 1.922 | 2.653 | 38 |
| $\mathrm{LaRhO_3}$ | $Pbnm$ (62) | 3.962 | 1 | 1.922 | 2.653 | 24 |
| $\mathrm{LaScO_3}$ | $Pbnm$ (62) | 4.053 | 1 | 1.922 | 2.653 | 23 |
| $\mathrm{LaTiO_3}$ | $Pnma$ (62) | 3.971 | 1 | 1.922 | 2.653 | 39 |
| $\mathrm{LaVO_3}$ | $P2_1/c$ (14) | 3.923 | 1 | 2.522 | 3.281 | 40 |
| $\mathrm{LaYbO_3}$ | $Pna2_1$ (33) | 4.186 | 1 | 2.322 | 3.307 | 41 |
| $\mathrm{NaNbO_3}$ | $Pbcm$ (57) | 3.903 | 1 | 2.722 | 3.558 | 42 |
| $\mathrm{NaTaO_3}$ | $Pnma$ (62) | 3.886 | 1 | 1.922 | 2.653 | 43 |
| $\mathrm{NdAlO_3}$ | $R\bar{3}c$ (167) | 3.767 | 1 | 1.371 | 1.686 | 44 |
| $\mathrm{NdNiO_3}$ | $Pbnm$ (62) | 3.806 | 1 | 1.922 | 2.653 | 37 |
| $\mathrm{NdRhO_3}$ | $Pbnm$ (62) | 3.919 | 1 | 1.922 | 2.653 | 24 |
| $\mathrm{NdScO_3}$ | $Pbnm$ (62) | 4.012 | 1 | 1.922 | 2.653 | 23 |
| $\mathrm{PbZrO_3}$ | $Pbam$ (55) | 4.145 | 1 | 2.922 | 3.780 | 45 |
| $\mathrm{PrAlO_3}$ | $R\bar{3}c$ (167) | 3.778 | 1 | 1.371 | 1.686 | 44 |
| $\mathrm{PrNiO_3}$ | $Pbnm$ (62) | 3.812 | 1 | 1.922 | 2.653 | 37 |
| $\mathrm{PrRhO_3}$ | $Pbnm$ (62) | 3.931 | 1 | 1.922 | 2.653 | 24 |
| $\mathrm{PrScO_3}$ | $Pnma$ (62) | 4.022 | 1 | 1.922 | 2.653 | 46 |
| $\mathrm{SmNiO_3}$ | $Pbnm$ (62) | 3.793 | 1 | 1.922 | 2.653 | 47 |

**Table S2:** Space groups and references for inorganic perovskite compounds. (continued)

**Ia Oxide-bridged inorganic perovskites** (continued)

| Compound | Space Group | ø B-B Dist. [Å] | A-Site Atom Count | $I_{\mathrm{G,comb}}$ [bit pos.$^{-1}$] | $I_{\mathrm{G,conf}}$ [bit pos.$^{-1}$ arity$^{-1}$] | Ref. |
|---|---|---|---|---|---|---|
| $SmRhO_3$ | *Pbnm* (62) | 3.898 | 1 | 1.922 | 2.653 | [24] |
| $SmScO_3$ | *Pbnm* (62) | 3.991 | 1 | 1.922 | 2.653 | [23] |
| $SrBiO_3$ | $P2_1/c$ (14) | 4.253 | 1 | 2.522 | 3.281 | [48] |
| $SrCoO_3$ | $Pm\bar{3}m$ (221) | 3.829 | 1 | 1.371 | 1.371 | [49] |
| $SrHfO_3$ | *Pnma* (62) | 4.070 | 1 | 1.922 | 2.653 | [50] |
| $SrNbO_3$ | *Pnma* (62) | 4.028 | 1 | 1.922 | 2.653 | [51] |
| $SrPbO_3$ | *Pnma* (62) | 4.174 | 1 | 1.922 | 2.653 | [52] |
| $SrRuO_3$ | *Pnma* (62) | 3.924 | 1 | 1.922 | 2.653 | [53] |
| $SrSnO_3$ | *Pnma* (62) | 4.028 | 1 | 1.922 | 2.653 | [54] |
| $SrTbO_3$ | *Pnma* (62) | 4.181 | 1 | 1.922 | 2.653 | [55] |
| $SrVO_3$ | $Pm\bar{3}m$ (221) | 3.843 | 1 | 1.371 | 1.371 | [56] |
| $SrZrO_3$ | *Pnma* (62) | 4.147 | 1 | 1.922 | 2.653 | [57] |
| $TbRhO_3$ | *Pbnm* (62) | 3.866 | 1 | 1.922 | 2.653 | [24] |
| $TbScO_3$ | *Pbnm* (62) | 3.959 | 1 | 1.922 | 2.653 | [23] |
| Mean | | 3.950 | 1.0 | 1.909 | 2.604 | |
| Median | | 3.944 | 1.0 | 1.922 | 2.653 | |

**Ib Halide-bridged inorganic perovskites**

| Compound | Space Group | ø B-B Dist. [Å] | A-Site Atom Count | $I_{\mathrm{G,comb}}$ [bit pos.$^{-1}$] | $I_{\mathrm{G,conf}}$ [bit pos.$^{-1}$ arity$^{-1}$] | Ref. |
|---|---|---|---|---|---|---|
| $CsHgF_3$ | $Pm\bar{3}m$ (221) | 4.570 | 1 | 1.371 | 1.371 | [58] |
| $CsPbBr_3$ | *Pnma* (62) | 5.861 | 1 | 1.922 | 2.653 | [59] |
| $CsPbCl_3$ | $P2_1/m$ (11) | 5.605 | 1 | 2.922 | 3.749 | [60] |
| $KAgF_3$ | *Pnma* (62) | 4.319 | 1 | 1.922 | 2.653 | [61] |
| $KCdF_3$ | *Pnma* (62) | 4.320 | 1 | 1.922 | 2.653 | [62] |
| $KCoF_3$ | $Pm\bar{3}m$ (221) | 4.071 | 1 | 1.371 | 1.371 | [63] |
| $KCrF_3$ | $C2/m$ (12) | 4.188 | 1 | 2.522 | 3.250 | [64] |
| $KCuF_3$ | $I4/mcm$ (140) | 4.071 | 1 | 1.922 | 2.187 | [65] |
| $KFeF_3$ | $Pm\bar{3}m$ (221) | 4.120 | 1 | 1.371 | 1.371 | [66] |
| $KHgF_3$* | *Cmmm* (65) | 4.410 | 1 | 1.922 | 1.922 | [58] |
| $KMgF_3$ | $Pm\bar{3}m$ (221) | 3.986 | 1 | 1.371 | 1.371 | [65] |
| $KMnF_3$ | $Pm\bar{3}m$ (221) | 4.185 | 1 | 1.371 | 1.371 | [67] |
| $KNiF_3$ | $Pm\bar{3}m$ (221) | 4.012 | 1 | 1.371 | 1.371 | [63] |
| $KVF_3$ | $Pm\bar{3}m$ (221) | 4.131 | 1 | 1.371 | 1.371 | [68] |
| $KZnF_3$ | $Pm\bar{3}m$ (221) | 4.055 | 1 | 1.371 | 1.371 | [63] |
| $RbCaF_3$ | $Pm\bar{3}m$ (221) | 4.445 | 1 | 1.371 | 1.371 | [69] |
| $RbHgF_3$ | $Pm\bar{3}m$ (221) | 4.470 | 1 | 1.371 | 1.371 | [58] |
| $RbVF_3$ | $Pm\bar{3}m$ (221) | 4.182 | 1 | 1.371 | 1.371 | [68] |
| Mean | | 4.389 | 1.0 | 1.674 | 1.897 | |
| Median | | 4.187 | 1.0 | 1.371 | 1.371 | |

* changed space group from *Pnma*

**Table S2:** Space groups and references for inorganic perovskite compounds. (continued 2)

### Ic Sulfide-bridged inorganic perovskites

| Compound | Space Group | ø B-B Dist. [Å] | A-Site Atom Count | $I_{\mathrm{G,comb}}$ [bit pos.$^{-1}$] | $I_{\mathrm{G,conf}}$ [bit pos.$^{-1}$ arity$^{-1}$] | Ref. |
|---|---|---|---|---|---|---|
| $BaUS_3$ | $Pnma$ (62) | 5.175 | 1 | 1.922 | 2.653 | 70 |
| $BaZrS_3$ | $Pnma$ (62) | 4.983 | 1 | 1.922 | 2.653 | 71 |
| $CaZrS_3$ | $Pnma$ (62) | 4.798 | 1 | 1.922 | 2.653 | 71 |
| $CeScS_3$ | $Pnma$ (62) | 4.819 | 1 | 1.922 | 2.653 | 72 |
| $CrUS_3$ | $Pnma$ (62) | 4.610 | 1 | 1.922 | 2.653 | 73 |
| $GdScS_3$ | $Pnma$ (62) | 4.743 | 1 | 1.922 | 2.653 | 74 |
| $UNiS_3$ | $Pnma$ (62) | 4.522 | 1 | 1.922 | 2.653 | 75 |
| $URhS_3$ | $Pnma$ (62) | 4.535 | 1 | 1.922 | 2.653 | 76 |
| $YScS_3$ | $Pna2_1$ (33) | 4.729 | 1 | 2.322 | 3.307 | 77 |
| Mean | | 4.768 | 1.0 | 1.966 | 2.726 | |
| Median | | 4.743 | 1.0 | 1.922 | 2.653 | |

**Table S3:** Space group and references for cyano-bridged perovskite compounds.

### II Cyano-Bridged Perovskites

| Compound | Space Group | ø B-B Dist. [Å] | A-Site Atom Count | $I_{\mathrm{G,comb}}$ [bit pos.$^{-1}$] | $I_{\mathrm{G,conf}}$ [bit pos.$^{-1}$ arity$^{-1}$] | Ref. |
|---|---|---|---|---|---|---|
| $Na_2Mn[Mn(CN)_6]$ | $R\bar{3}$ (148) | 4.990 | 1 | 1.936 | 2.674 | 78 |
| $K_2Mn[Mn(CN)_6]$ | $P2_1/c$ (14) | 5.089 | 1 | 3.125 | 3.968 | 79 |
| $Rb_2Mn[Mn(CN)_6]$ | $P2_1/c$ (14) | 5.191 | 1 | 3.125 | 3.968 | 79 |
| $Cs_2Mn[Mn(CN)_6]$ | $Fm\bar{3}m$ (225) | 5.303 | 1 | 1.936 | 2.336 | 79 |
| Mean | | 5.143 | 1.0 | 2.531 | 3.237 | |
| Median | | 5.140 | 1.0 | 2.531 | 3.321 | |

**Table S4:** Space groups and references for borate-bridged perovskite compounds.

### III Borate-Bridged Perovskites

| Compound | Space Group | ø B-B Dist. [Å] | A-Site Atom Count | $I_{\mathrm{G,comb}}$ [bit pos.$^{-1}$] | $I_{\mathrm{G,conf}}$ [bit pos.$^{-1}$ arity$^{-1}$] | Ref. |
|---|---|---|---|---|---|---|
| $Cs[Sr(BH_4)_3]$ | $P2_12_12$ (18) | 5.888 | 1 | 3.264 | 4.215 | 80 |
| $K[Sr(BH_4)_3]$ | $Pna2_1$ (33) | 5.738 | 1 | 4.087 | 5.073 | 80 |
| $Rb[Sr(BH_4)_3]$ | $Pna2_1$ (33) | 5.813 | 1 | 4.087 | 5.073 | 80 |
| $(NH_4)[Ca(BH_4)_3]$ | $P\bar{4}3m$ (215) | 5.623 | 5 | 1.736 | 2.178 | 81 |
| $(H_2dabco)[Na(BF_4)_3]$ | $Pa\bar{3}$ (205) | 6.996 | 22 | 3.898 | 4.382 | 82 |
| $(H_2dabco)[K(BF_4)_3]$ | $Pa\bar{3}$ (205) | 7.039 | 22 | 3.898 | 4.382 | 83 |
| Mean | | 6.183 | 8.7 | 3.495 | 4.217 | |
| Median | | 5.851 | 3.0 | 3.898 | 4.382 | |

**Table S5:** Space groups and references for formate-bridged perovskite compounds.

**IV Formate-Bridged Perovskites**

| Compound | Space Group | ø B-B Dist. [Å] | A-Site Atom Count | $I_{\mathrm{G,comb}}$ [bit pos.$^{-1}$] | $I_{\mathrm{G,conf}}$ [bit pos.$^{-1}$ arity$^{-1}$] | Ref. |
|---|---|---|---|---|---|---|
| $(NH_4)[Cd(HCOO)_3]$ | $Pna2_1$ (33) | 5.623 | 5 | 4.170 | 5.155 | 84 |
| $K[Co(HCOO)_3]$ | $P6_322$ (182) | 5.853 | 1 | 2.020 | 2.535 | 85 |
| $Na[Mn(HCOO)_3]$ | $P2_13$ (198) | 5.594 | 1 | 2.449 | 3.171 | 8 |
| $K[Mn(HCOO)_3]$ | $C2/c$ (15) | 5.893 | 1 | 3.093 | 3.963 | 8 |
| $(MA)[Co(HCOO)_3]$ | $Pnma$ (62) | 5.802 | 8 | 3.726 | 4.569 | 86 |
| $(MA)[Mn(HCOO)_3]$ | $Pnma$ (62) | 5.949 | 8 | 3.726 | 4.569 | 87 |
| $(AZ)[Mn(HCOO)_3]$ | $P2_1/c$ (14) | 6.174 | 12 | 5.644 | 6.629 | 87 |
| $(Hy)[Mn(HCOO)_3]$ | $Pna2_1$ (33) | 5.917 | 7 | 4.322 | 5.307 | 88 |
| $(Hy)[Zn(HCOO)_3]$ | $Pna2_1$ (33) | 5.789 | 7 | 4.322 | 5.307 | 88 |
| $(Hy)[Mg(HCOO)_3]$ | $P2_12_12_1$ (19) | 5.883 | 7 | 4.322 | 5.307 | 88 |
| $(Hy)[Co(HCOO)_3]$ | $P2_12_12_1$ (19) | 5.879 | 7 | 4.322 | 5.307 | 88 |
| $(Gua)[Cd(HCOO)_3]$ | $R\bar{3}c$ (167) | 6.226 | 10 | 2.555 | 3.125 | 89 |
| $(FA)[Mn(HCOO)_3]$ | $C2/c$ (15) | 6.034 | 8 | 3.630 | 4.529 | 90 |
| $(AZ)[Cu(HCOO)_3]^*$ | $P2_1/c$ (14) | 6.062 | 12 | 4.684 | 5.623 | 91 |
| $(EA)[Mn(HCOO)_3]$ | $Pna2_1$ (33) | 6.076 | 11 | 4.585 | 5.570 | 87 |
| $(EA)[Mg(HCOO)_3]$ | $Pna2_1$ (33) | 5.961 | 11 | 4.585 | 5.570 | 92 |
| $(EA)[Cu(HCOO)_3]$ | $Pna2_1$ (33) | 5.971 | 11 | 4.585 | 5.570 | 93 |
| $(HIm)[Mn(HCOO)_3]$ | $P2_1/c$ (14) | 6.277 | 10 | 5.524 | 6.509 | 94 |
| $(Ace)[Mn(HCOO)_3]$ | $P2_1/n$ (14) | 6.163 | 11 | 4.585 | 5.570 | 95 |
| $(DMHy)[Mn(HCOO)_3]$ | $P2_1/n$ (14) | 6.218 | 13 | 4.700 | 5.686 | 96 |
| Mean | | 5.967 | 8.1 | 4.077 | 4.979 | |
| Median | | 5.955 | 8.0 | 4.322 | 5.307 | |

**Table S6:** Space groups and references for azido-bridged perovskite compounds.

**V Azido-Bridged Perovskites**

| Compound | Space Group | ø B-B Dist. [Å] | A-Site Atom Count | $I_{\mathrm{G,comb}}$ [bit pos.$^{-1}$] | $I_{\mathrm{G,conf}}$ [bit pos.$^{-1}$ arity$^{-1}$] | Ref. |
|---|---|---|---|---|---|---|
| $(MA)[Mn(N_3)_3]$ | $P2_1/c$ (14) | 6.072 | 8 | 4.225 | 5.147 | 97 |
| $(DMA)[Mn(N_3)_3]$ | $P2_1$ (4) | 6.240 | 11 | 4.392 | 5.363 | 97 |
| $(TrMA)[Mn(N_3)_3]$ | $P2_1/c$ (14) | 6.306 | 14 | 4.668 | 5.558 | 97 |
| $(TrMA)[Cd(N_3)_3]$ | $P2_1/c$ (14) | 6.412 | 14 | 4.668 | 5.558 | 98 |
| $(TeMA)[Cd(N_3)_3]$ | $C2/c$ (15) | 6.460 | 17 | 3.866 | 4.795 | 99 |
| $(DMEA)[Mn(N_3)_3]$ | $Cc$ (9) | 6.516 | 17 | 4.755 | 5.726 | 100 |
| $(CPrA)[Mn(N_3)_3]$ | $Pbca$ (61) | 6.337 | 12 | 4.459 | 5.305 | 101 |
| Mean | | 6.335 | 13.0 | 4.433 | 5.350 | |
| Median | | 6.337 | 14.0 | 4.459 | 5.363 | |

**Table S7:** Space groups and references for hypophosphite-bridged perovskite compounds.

**VI Hypophosphite Perovskites**

| Compound | Space Group | ø B-B Dist. [Å] | A-Site Atom Count | $I_{\mathrm{G,comb}}$ [bit pos.$^{-1}$] | $I_{\mathrm{G,conf}}$ [bit pos.$^{-1}$ arity$^{-1}$] | Ref. |
|---|---|---|---|---|---|---|
| (FA)[Mn(H$_2$POO)$_3$] | $P2_1/c$ (14) | 6.505 | 8 | 4.585 | 5.570 | 102 |
| (Gua)[Mn(H$_2$POO)$_3$]* | $C2/m$ (12) | 6.557 | 10 | 4.008 | 4.961 | 102 |
| (HIm)[Mn(H$_2$POO)$_3$] | $P2_1/c$ (14) | 6.605 | 10 | 5.700 | 6.686 | 102 |
| (TrAz)[Mn(H$_2$POO)$_3$] | $P2_1/c$ (14) | 6.636 | 9 | 4.644 | 5.629 | 102 |
| (MHy)[Mn(H$_2$POO)$_3$]* | $Pnma$ (62) | 6.395 | 10 | 4.008 | 4.857 | 103 |
| (DMA)[Mn(H$_2$POO)$_3$] | $P2_1/c$ (14) | 6.670 | 11 | 6.340 | 7.325 | 104 |
| Mean | | 6.561 | 9.7 | 4.881 | 5.838 | |
| Median | | 6.581 | 10.0 | 4.615 | 5.600 | |

**Table S8:** Space groups and references for hybrid organic-inorganic perovskite (HOIP) compounds.

**VII Hybrid Organic-Inorganic Perovskites**

| Compound | Space Group | ø B-B Dist. [Å] | A-Site Atom Count | $I_{\mathrm{G,comb}}$ [bit pos.$^{-1}$] | $I_{\mathrm{G,conf}}$ [bit pos.$^{-1}$ arity$^{-1}$] | Ref. |
|---|---|---|---|---|---|---|
| (MA)[PbI$_3$] | $Pnma$ (62) | 6.217 | 8 | 3.085 | 3.913 | 11 |
| deuterated (MA)[GeCl$_3$] | $P2_1/c$ (14) | 5.516 | 8 | 3.585 | 4.570 | 9 |
| (MHy)[PbCl$_3$] | $P2_1$ (4) | 5.747 | 10 | 4.807 | 5.778 | 105 |
| (3 AP)[RbBr$_3$] | $Cc$ (9) | 6.590 | 18 | 4.459 | 5.430 | 106 |
| (PIP)[NaI$_3$] | $C2/c$ (15) | 6.620 | 18 | 3.550 | 4.475 | 107 |
| (H$_2$dabco)[RbCl$_3$] | $P3_221$ (154) | 6.552 | 22 | 4.739 | 5.649 | 108 |
| (H$_2$dabco)[CsCl$_3$] | $C2/c$ (15) | 6.678 | 22 | 6.710 | 7.689 | 108 |
| (H$_2$dabco)[RbBr$_3$] | $P3_221$ (154) | 6.784 | 22 | 4.739 | 5.649 | 109 |
| (MDABCO)[RbI$_3$] | $R3:R$ (146) | 7.272 | 25 | 3.546 | 4.546 | 109 |
| Mean | | 6.442 | 17.0 | 4.358 | 5.300 | |
| Median | | 6.590 | 18.0 | 4.459 | 5.430 | |

**Table S9:** Space groups and references for thiocyanato-bridged perovskite compounds.

**VIII Thiocyanato-Bridged Perovskites**

| Compound | Space Group | ø B-B Dist. [Å] | A-Site Atom Count | $I_{\mathrm{G,comb}}$ [bit pos.$^{-1}$] | $I_{\mathrm{G,conf}}$ [bit pos.$^{-1}$ arity$^{-1}$] | Ref. |
|---|---|---|---|---|---|---|
| Cs[Cd(SCN)$_3$] | $P2_1/c$ (14) | 6.399 | 1 | 3.550 | 4.432 | 110 |
| (Me$_3$S)[Cd(SCN)$_3$] | $Pa\bar{3}$ (205) | 6.874 | 13 | 3.120 | 3.592 | 111 |
| Mean | | 6.637 | 7.0 | 3.335 | 4.012 | |
| Median | | 6.637 | 7.0 | 3.335 | 4.012 | |

**Table S10:** Space groups and references for metal free perovskite compounds.

**IX Metal Free Perovskites**

| Compound | Space Group | ø B-B Dist. [Å] | A-Site Atom Count | $I_{\mathrm{G,comb}}$ [bit pos.$^{-1}$] | $I_{\mathrm{G,conf}}$ [bit pos.$^{-1}$ arity$^{-1}$] | Ref. |
|---|---|---|---|---|---|---|
| *rac*−3 AQ−$NH_4Cl_3$ | $P2_1$ (4) | 6.737 | 25 | 5.044 | 6.015 | 112 |
| *rac*−3 AQ−$NH_4Br_3$ | $P2_1$ (4) | 6.912 | 25 | 5.044 | 6.015 | 112 |
| *S*−3 AQ−$NH_4Cl_3$ | $P2_1$ (4) | 6.760 | 25 | 5.044 | 6.015 | 112 |
| *S*−3 AQ−$NH_4Br_3$ | $P2_1$ (4) | 6.905 | 25 | 5.044 | 6.015 | 112 |
| *R*−3 AQ−$NH_4Cl_3$ | $P2_1$ (4) | 6.747 | 25 | 5.044 | 6.015 | 112 |
| *R*−3 AQ−$NH_4Br_3$ | $P2_1$ (4) | 6.905 | 25 | 5.044 | 6.015 | 112 |
| *rac*−3 AP−$NH_4Cl_3$ | $Cc$ (9) | 6.344 | 18 | 4.700 | 5.671 | 112 |
| *rac*−3 AP−$NH_4Br_3$ | $Cc$ (9) | 6.567 | 18 | 4.700 | 5.671 | 112 |
| *S*−3 AP−$NH_4Cl_3$ | $P2_1$ (4) | 6.386 | 18 | 5.700 | 6.671 | 112 |
| *S*−3 AP−$NH_4Br_3$ | $P2_1$ (4) | 6.605 | 18 | 5.700 | 6.671 | 112 |
| *R*−3 AP−$NH_4Cl_3$ | $P2_1$ (4) | 6.383 | 18 | 5.700 | 6.671 | 112 |
| *R*−3 AP−$NH_4Br_3$ | $P2_1$ (4) | 6.599 | 18 | 5.700 | 6.671 | 112 |
| ODABCO−$NH_4Cl_3$ | $Pca2_1$ (29) | 6.621 | 23 | 4.954 | 5.939 | 112 |
| MDABCO−$NH_4I_3$ | $R3$ (146) | 7.259 | 25 | 3.748 | 4.748 | 112 |
| $H_2$dabco−$NH_4Br_3$ | $P3_121$ (152) | 6.742 | 22 | 4.940 | 5.851 | 112 |
| Mean | | 6.698 | 21.9 | 5.074 | 6.044 | |
| Median | | 6.737 | 23.0 | 5.044 | 6.015 | |

**Table S11:** Space groups and references for perchlorate-bridged perovskite compounds.

**X Perchlorate Perovskites**

| Compound | Space Group | ø B-B Dist. [Å] | A-Site Atom Count | $I_{\mathrm{G,comb}}$ [bit pos.$^{-1}$] | $I_{\mathrm{G,conf}}$ [bit pos.$^{-1}$ arity$^{-1}$] | Ref. |
|---|---|---|---|---|---|---|
| $(H_2hpz)[K(ClO_4)_3]$ | $Pbca$ (61) | 7.203 | 21 | 5.209 | 6.055 | 113 |
| $(PIP)[Na(ClO_4)_3]$ | $P2_1/c$ (14) | 6.911 | 18 | 5.087 | 6.073 | 114 |
| $(H_2dabco)[Na(ClO_4)_3]$ | $Pa\bar{3}$ (205) | 7.077 | 22 | 3.898 | 4.382 | 115 |
| $(H_2dabco)[Rb(ClO_4)_3]$ | $Pa\bar{3}$ (205) | 7.226 | 22 | 3.898 | 4.382 | 115 |
| $(H_2dabco)[K(ClO_4)_3]$ | $Pa\bar{3}$ (205) | 7.146 | 22 | 3.898 | 4.382 | 115 |
| $(ODABCO)[K(ClO_4)_3]$ | $P2_1/c$ (14) | 7.281 | 23 | 5.311 | 6.267 | 116 |
| $(PIP)[Na(ClO_4)_3]$ | $P2_1/c$ (14) | 6.882 | 18 | 5.087 | 6.073 | 116 |
| Mean | | 7.104 | 20.9 | 4.627 | 5.373 | |
| Median | | 7.146 | 22.0 | 5.087 | 6.055 | |

**Table S12:** Space groups and references for dicyanamide-bridged perovskite compounds.

**XI Dicyanamide-Bridged Perovskites**

| Compound | Space Group | ø B-B Dist. [Å] | A-Site Atom Count | $I_{\mathrm{G,comb}}$ [bit pos.$^{-1}$] | $I_{\mathrm{G,conf}}$ [bit pos.$^{-1}$ arity$^{-1}$] | Ref. |
|---|---|---|---|---|---|---|
| (BTba)[Mn(dca)$_3$] | *Pnma* (62) | 8.881 | 54 | 5.301 | 6.157 | [117] |
| (BTba)[Co(dca)$_3$] | *Pnma* (62) | 8.784 | 54 | 5.301 | 6.157 | [117] |
| (BTea)[Mn(dca)$_3$] | *Pnma* (62) | 8.305 | 36 | 4.893 | 5.746 | [117] |
| (BTea)[Fe(dca)$_3$] | *Pnma* (62) | 8.240 | 36 | 4.893 | 5.746 | [117] |
| (TrPrMA)[Co(dca)$_3$] | *R*3*c* (161) | 8.156 | 35 | 4.181 | 5.099 | unpublished |
| (TrPrMA)[Ni(dca)$_3$] | *R*3*c* (161) | 8.108 | 35 | 4.181 | 5.099 | unpublished |
| (TrPrMA)[Mn(dca)$_3$] | *R*3*c* (161) | 8.247 | 35 | 4.181 | 5.099 | unpublished |
| [Et$_3$(n−Pr)P][Cd(dca)$_3$] | $P2_1/c$ (14) | 8.451 | 32 | 5.585 | 6.570 | [118] |
| [Et$_3$(CH$_2$OCH$_3$)P][Mn(dca)$_3$] | $P2_1/c$ (14) | 8.238 | 30 | 5.524 | 6.509 | [119] |
| [Et$_3$(n−Pr)P][Mn(dca)$_3$] | $P2_12_12_1$ (19) | 8.271 | 32 | 5.585 | 6.570 | [119] |
| [Et$_3$(CH$_2$CHCH$_2$)P][Mn(dca)$_3$] | $P2_1/c$ (14) | 8.198 | 30 | 5.524 | 6.509 | [119] |
| [Et$_3$P(CH$_2$)$_2$Cl][Mn(dca)$_3$] | $P2_1/c$ (14) | 8.175 | 29 | 5.492 | 6.477 | [120] |
| [EtPh$_3$P][Cd(dca)$_3$] | $P2_1/c$ (14) | 8.789 | 41 | 5.833 | 6.818 | [121] |
| Mean | | 8.373 | 36.8 | 5.113 | 6.043 | |
| Median | | 8.247 | 35.0 | 5.301 | 6.157 | |

**Table S13:** Space groups and references for dicyanoaurate-bridged perovskite compounds.

**XII Dicyanoaurate-Bridged Perovskites**

| Compound | Space Group | ø B-B Dist. [Å] | A-Site Atom Count | $I_{\mathrm{G,comb}}$ [bit pos.$^{-1}$] | $I_{\mathrm{G,conf}}$ [bit pos.$^{-1}$ arity$^{-1}$] | Ref. |
|---|---|---|---|---|---|---|
| (PPN)[Mn[Au(CN)$_2$]$_3$] | $C2/c$ (15) | 10.415 | 69 | 5.445 | 6.412 | 122 |
| (PPN)[Cd[Au(CN)$_2$]$_3$] | $C2/c$ (15) | 11.249 | 69 | 5.445 | 6.412 | 122 |
| (PPN)[Ni(Au(CN)$_2$)$_3$] | $R\bar{3}c$ (167) | 10.270 | 69 | 3.958 | 4.647 | 123 |
| Mean | | 10.645 | 69.0 | 4.949 | 5.824 | |
| Median | | 10.415 | 69.0 | 5.445 | 6.412 | |

# 3 Thiocyanates

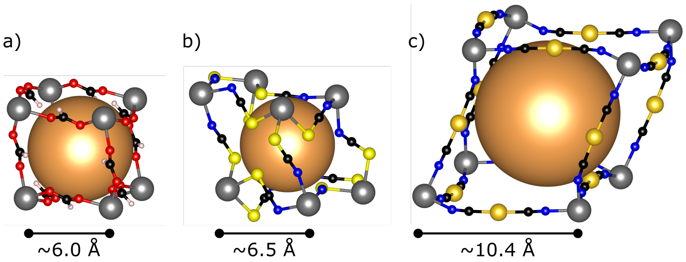

**Figure S3:** Schematic of three different molecular perovskites, (a) $AB(\mathrm{HCOO})_3$ formates, (b) $AB(\mathrm{SCN})_3$ thiocyanates and (c) $AB([\mathrm{Au(CN)}_2])_3$ dicyanoaurates with the molecular $A$-site cation shown as orange space-filling sphere for clarity. For thiocyanates, the relatively large distortion of the pseudocubic $\mathrm{ReO}_3$ network compared to formates and dicyanoaurates is apparent. Color-code: red - oxygen, black - carbon, grey - $B^{2+}$ metal, yellow - sulfur, blue - nitrogen, light orange - gold.

# 4 Case Study: Columnar Shifts

All combinations of no shift, zone-center (neighboring columns shift in the same direction), and zone-boundary shifts (alternating patterns with doubled repeat units) are applied to a generic molecular perovskite with hypothetical three-atom linker and monoatomic A-site cation. Octahedra are assumed to remain undistorted. Furthermore, the case study is simplified to two dimensions for better visualization. Wyckoff positions that are used for the calculation of the discussed complexity values are shown in Figure S4 with respect to the 2D-projected perovskites' plane groups. Detailed results are reported in Table S14.

## 4.1 Visualization of Calculation Principle

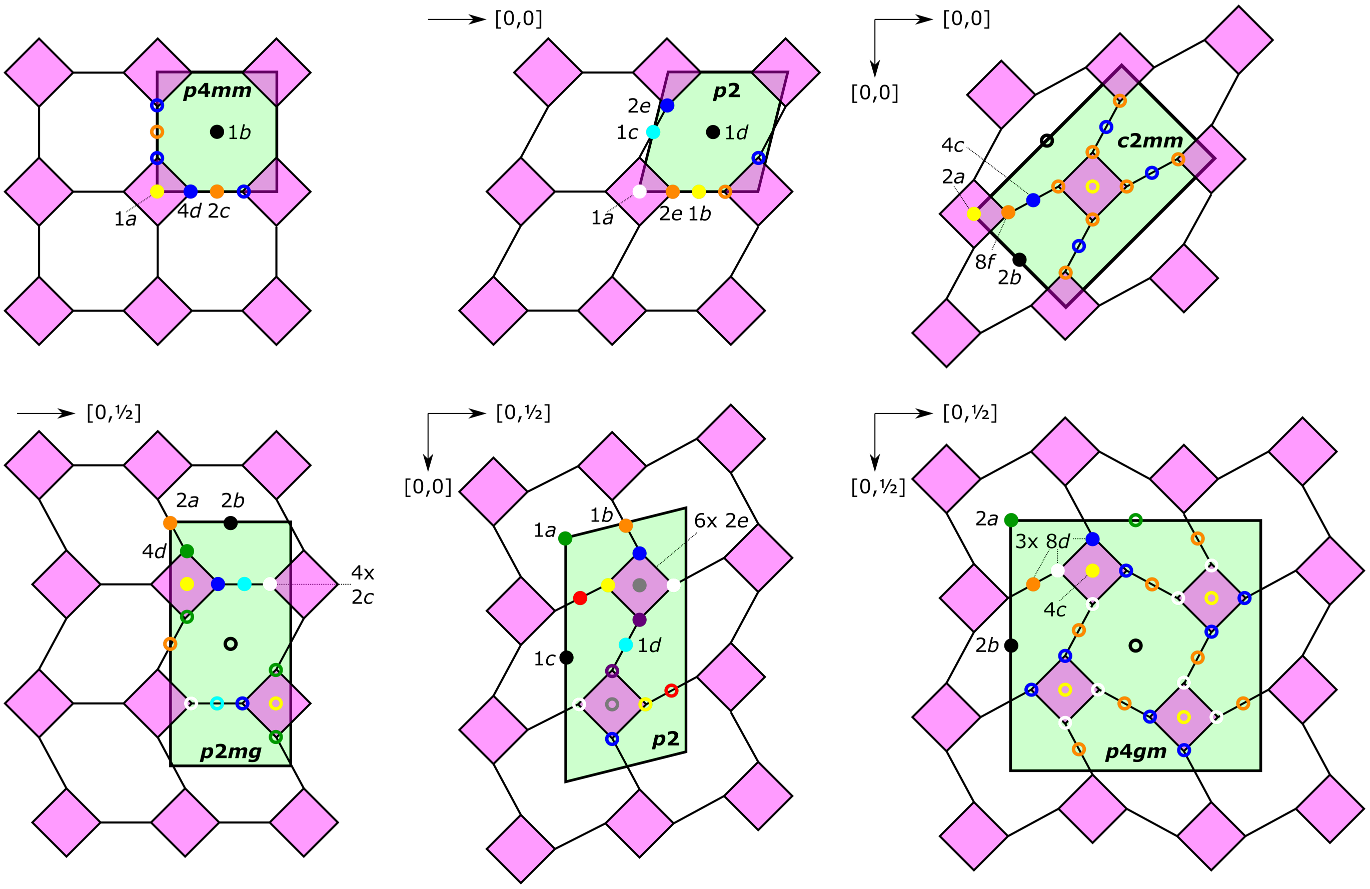

**Figure S4:** Six two-dimensional, columnar shift systems for molecular perovskites. Zone-center: k = [0,0]. Zone-boundary: k = [0,$\frac{1}{2}$]. Wyckoff positions that are used as a basis for combinatorial complexity calculations are marked with colored dots. Their symmetry equivalent positions are depicted as open circles of the same color. Regardless of how many positions are overlapping in the projection, only one of the positions with identical 2D-coordinates is considered here. For example, the position 1*a* in the unshifted perovskite could portray the B-site, an octahedral vertex, or even the third linker atom, but is only considered once in the calculation. Arities, which are additionally required for configurational complexity calculations, are not explicitly featured but can be assigned to given Wyckoff positions easily. Keep in mind that reduced unit cells are the basis for complexity calculations, which can change the ratio between multiplicities and arities compared to the standard unit cells that are shown here. This is relevant for *c*2*mm* due to its non-primitive centering. Figure adapted from ref.[124]

## 4.2 Detailed Results

**Table S14:** Complexity Parameters in dependence of columnar shifts, calculated for 2D-projected generic molecular perovskites.

| $I_{\mathrm{G,comb}}$ [bit pos.$^{-1}$] | a-shifts inactive | a: zone-center k = [0,0] | a: zone-boundary k = [0,$\frac{1}{2}$] |
|---|---|---|---|
| b: inactive | 1.750 | 2.500 | 2.750 |
| b: k = [0,0] | 2.500 | 1.750 | 3.250 |
| b: k = [0,$\frac{1}{2}$] | 2.750 | 3.250 | 2.375 |

| $I_{\mathrm{G,conf}}$ [bit pos.$^{-1}$ arity$^{-1}$] | a-shifts inactive | a: zone-center k = [0,0] | a: zone-boundary k = [0,$\frac{1}{2}$] |
|---|---|---|---|
| b: inactive | 2.059 | 2.918 | 3.459 |
| b: k = [0,0] | 2.918 | 2.122 | 3.950 |
| b: k = [0,$\frac{1}{2}$] | 3.459 | 3.950 | 2.978 |

# 5 Abbreviations

| | |
|---|---|
| Ace | acetamidinium |
| 3AP | 3-ammoniopyrrolidinium |
| 3AQ | 3-ammonioquinuclidinium |
| AZ | azetidinium, cyclotrimethyleneammonium |
| BTba | benzyltributylammonium |
| BTea | benzyltriethylammonium |
| CPrA | cyclopropylammonium |
| dabco | 1,4-diazabicyclo[2.2.2]octane |
| dca | dicyanamide |
| DMA | dimethylammonium |
| DMEA | dimethylethylaminium |
| DMHy | dimethylhydrazinium |
| EA | ethylammonium |
| FA | formamidinium |
| Gua | guanidinium |
| hpz | homopiperazine |
| Hy | hydrazinium |
| Im | imidazole |
| MA | methylammonium |
| MDABCO | *N*-methyl-*N'*-diazabicyclo[2.2.2]octonium |
| MHy | methylhydrazinium |
| ODABCO | *N*-hydroxy-*N'*-diazabicyclo[2.2.2]octonium |
| PIP | piperazinium |
| Ph | phenyl |
| Pr | propyl |
| PPN | bis(triphenylphosphoranylidene)ammonium |
| TeMA | tetramethylammonium |
| TrAZ | triazolium |
| TrMA | trimethylammonium |
| TrPrMA | tripropylmethylammonium |

# 6 Supplementary References

[1] W. Hornfeck, *Acta Cryst*, 2020, **76**, 534–548.

[2] C. Kaussler and G. Kieslich, *J. Appl. Cryst.*, 2021, **54**, 306–316.

[3] W. H. Baur, E. Tillmanns and W. Hofmeister, *Acta Cryst. B*, 1983, **39**, 669–674.

[4] J. Dshemuchadse and W. Steurer, *Inorg. Chem.*, 2015, **54**, 1120–1128.

[5] S. V. Krivovichev, *Angew. Chem. Int. Ed.*, 2014, **53**, 654–61.

[6] Y. Ren, I. W. H. Oswald, X. Wang, G. T. McCandless and J. Y. Chan, *Cryst. Growth Des.*, 2016, **16**, 2945–2951.

[7] A. Antsyshkina, M. Porai Koshits, V. Ostrikova and G. Sadikov, *Sov. J. Coord. Chem*, 1983, **9**, 855–858.

[8] E. Eikeland, N. Lock, M. Filso, M. Stingaciu, Y. Shen, J. Overgaard and B. B. Iversen, *Inorg. Chem.*, 2014, **53**, 10178–10188.

[9] K. Yamada, K. Mikawa, T. Okuda and K. S. Knight, *J. Chem. Soc., Dalton Trans.*, 2002, 2112–2118.

[10] P. S. Whitfield, N. Herron, W. E. Guise, K. Page, Y. Q. Cheng, I. Milas and M. K. Crawford, *Sci. Rep.*, 2016, **6**, 35685.

[11] M. T. Weller, O. J. Weber, P. F. Henry, A. M. Di Pumpo and T. C. Hansen, *Chem. Commun.*, 2015, **51**, 4180–4183.

[12] G. H. Kwei, A. C. Lawson, S. J. L. Billinge and S. W. Cheong, *J. Phys. Chem.*, 1993, **97**, 2368–2377.

[13] R. Ali and M. Yashima, *J. Solid State Chem.*, 2005, **178**, 2867–2872.

[14] A. M. Glazer and S. A. Mabud, *Acta Crystallogr. B*, 1978, **34**, 1065–1070.

[15] A. A. Belik, M. Azuma, T. Saito, Y. Shimakawa and M. Takano, *Chem. Mater.*, 2005, **17**, 269–273.

[16] A. W. Hewat, *J. Phys. C: Solid State Phys.*, 1973, **6**, 2559–2572.

[17] K. Tsuda and M. Tanaka, *Acta Crystallogr. A*, 1995, **51**, 7–19.

[18] A. Palewicz, R. Przenioslo, I. Sosnowska and A. W. Hewat, *Acta Crystallogr. B*, 2007, **63**, 537–544.

[19] H. Müller-Buschbaum and C. Teske, *Z. anorg. allg. Chem.*, 1969, **369**, 255–264.

[20] N. L. Ross, J. Zhao and R. J. Angel, *J. Solid State Chem.*, 2004, **177**, 1276–1284.

[21] *J. Solid State Chem.*, 2004, **177**, 1667–1671.

[22] H. F. Kay and J. L. Miles, *Acta Crystallogr.*, 1957, **10**, 213–218.

[23] R. P. Liferovich and R. H. Mitchell, *J. Solid State Chem.*, 2004, **177**, 2188–2197.

[24] R. B. Macquart, M. D. Smith and H.-C. zur Loye, *Cryst. Growth Des.*, 2006, **6**, 1361–1365.

[25] M. Faucher and P. Caro, *Mater. Res. Bull.*, 1975, **10**, 1–7.

[26] J. Blasco, J. Stankiewicz and J. García, *J. Solid State Chem.*, 2006, **179**, 898–908.

[27] S. Ananyan, E. Antipov, V. Antonov, P. Arsen'ev, K. S. Bagdasarov, A. Kevorkyan, L. Kovba and A. Rakhmatulin, *Zh. Neorg. Khim.*, 1987, **32**, 2087–2091.

[28] C. J. Howard, B. J. Kennedy and B. C. Chakoumakos, *J. Phys. Condens. Matter*, 1999, **12**, 349–365.

[29] O. Haas, R. Struis and J. McBreen, *J. Solid State Chem.*, 2004, **177**, 1000–1010.

[30] J. Yang, *Acta Crystallogr. B*, 2008, **64**, 281–286.

[31] J.-S. Zhou, L. G. Marshall and J. B. Goodenough, *Phys. Rev. B*, 2014, **89**, 245138.

[32] H. Müller-Buschbaum and P.-H. Graebner, *Z. anorg. allg. Chem.*, 1971, **386**, 158–162.

[33] C. A. Dixon, C. M. Kavanagh, K. S. Knight, W. Kockelmann, F. D. Morrison and P. Lightfoot, *J. Solid State Chem.*, 2015, **230**, 337–342.

[34] L. Vasylechko, M. Berkowski, A. Matkovski, D. Savytskii and J. Fink-Finowicki, *Mater. Res. Bull.*, 2000, **35**, 333–340.

[35] H. M. Park, H. J. Lee, S. H. Park and H. I. Yoo, *Acta Crystallogr. C*, 2003, **59**, i131–i132.

[36] J. Rodríguez-Carvajal, M. Hennion, F. Moussa, A. H. Moudden, L. Pinsard and A. Revcolevschi, *Phys. Rev. B*, 1998, **57**, R3189–R3192.

[37] J. L. García-Muñoz, J. Rodríguez-Carvajal, P. Lacorre and J. B. Torrance, *Phys. Rev. B*, 1992, **46**, 4414–4425.

[38] S.-J. Kim, S. Lemaux, G. Demazeau, J.-Y. Kim and J.-H. Choy, *J. Am. Chem. Soc.*, 2001, **123**, 10413–10414.

[39] M. Cwik, T. Lorenz, J. Baier, R. Müller,

G. André, F. Bourée, F. Lichtenberg, A. Freimuth, R. Schmitz, E. Müller-Hartmann and M. Braden, *Phys. Rev. B*, 2003, **68**, 060401.

[40] P. Bordet, C. Chaillout, M. Marezio, Q. Huang, A. Santoro, S.-W. Cheong, H. Takagi, C. Oglesby and B. Batlogg, *J. Solid State Chem.*, 1993, **106**, 253–270.

[41] H. Müller-Buschbaum and C. Teske, *Z. anorg. allg. Chem.*, 1969, **369**, 255–264.

[42] D. O. Mishchuk, O. I. V'yunov, O. V. Ovchar and A. G. Belous, *Inorg. Mater.*, 2004, **40**, 1324–1330.

[43] M. Ahtee and L. Unonius, *Acta Crystallogr. A*, 1977, **33**, 150–154.

[44] C. J. Howard, B. J. Kennedy and B. C. Chakoumakos, *J. Phys. Condens. Matter*, 1999, **12**, 349–365.

[45] K. Yamasaki, Y. Soejima and K. F. Fischer, *Acta Crystallogr. B*, 1998, **54**, 524–530.

[46] T. M. Gesing, R. Uecker and J.-C. Buhl, *Z. Kristallogr. NCS*, 2009, **224**, 385–386.

[47] P. F. Henry, M. T. Weller and C. C. Wilson, *Chem. Mat.*, 2002, **14**, 4104–4110.

[48] S. M. Kazakov, C. Chaillout, P. Bordet, J. J. Capponi, M. Nunez-Regueiro, A. Rysak, J. L. Tholence, P. G. Radaelli, S. N. Putilin and E. V. Antipov, *Nature*, 1997, **390**, 148–150.

[49] Y. Long, Y. Kaneko, S. Ishiwata, Y. Taguchi and Y. Tokura, *J. Phys. Condens. Matter*, 2011, **23**, 245601.

[50] B. J. Kennedy, C. J. Howard and B. C. Chakoumakos, *Phys. Rev. B*, 1999, **60**, 2972–2975.

[51] H. Hannerz, G. Svensson, S. Istomin and O. D'yachenko, *J. Solid State Chem.*, 1999, **147**, 421–428.

[52] H.-L. Keller, K.-H. Meier and H. Müller-Buschbaum, *Z. Naturforsch. B*, 1975, **30**, 277–278.

[53] C. Bansal, H. Kawanaka, R. Takahashi and Y. Nishihara, *J. Alloys Compd.*, 2003, **360**, 47–53.

[54] M. Green, K. Prassides, P. Day and D. Neumann, *Int. J. Inorg. Chem.*, 2000, **2**, 35–41.

[55] K. Tezuka, M. Itoh, M. Haga and Y. Hinatsu, Materials Science Forum, 1999, pp. 578–585.

[56] Y. Lan, X. Chen and M. He, *J. Alloys Compd.*, 2003, **354**, 95–98.

[57] B. J. Kennedy, C. J. Howard and B. C. Chakoumakos, *Phys. Rev. B*, 1999, **59**, 4023–4027.

[58] R. Hoppe and R. Homann, *Z. anorg. allg. Chem.*, 1969, **369**, 212–216.

[59] C. C. Stoumpos, C. D. Malliakas, J. A. Peters, Z. Liu, M. Sebastian, J. Im, T. C. Chasapis, A. C. Wibowo, D. Y. Chung, A. J. Freeman, B. W. Wessels and M. G. Kanatzidis, *Cryst. Growth Des.*, 2013, **13**, 2722–2727.

[60] Y. Fujii, S. Hoshino, Y. Yamada and G. Shirane, *Phys. Rev. B*, 1974, **9**, 4549–4559.

[61] R.-H. Odenthal and R. Hoppe, *Monatsh. Chem.*, 1971, **102**, 1340–1350.

[62] Hidaka, M. and Hosogi, S., *J. Phys. France*, 1982, **43**, 1227–1232.

[63] K. Knox, *Acta Crystallogr.*, 1961, **14**, 583–585.

[64] S. Margadonna and G. Karotsis, *J. Am. Chem. Soc.*, 2006, **128**, 16436–16437.

[65] P. C. Burns, F. C. Hawthorne, A. M. Hofmeister and S. L. Moret, *Phys. Chem. Miner.*, 1996, **23**, 141–150.

[66] N. Miyata, K. Tanaka and F. Marumo, *Acta Crystallogr. B*, 1983, **39**, 561–564.

[67] Y. Ivanov, T. Nimura and K. Tanaka, *Acta Crystallogr. B*, 2004, **60**, 359–368.

[68] R. Williamson and W. Boo, *Inorg. Chem.*, 1977, **16**, 646–648.

[69] J. Hutton and R. J. Nelmes, *J. Phys. C: Solid State Phys.*, 1981, **14**, 1713–1736.

[70] A. Mesbah and J. A. Ibers, *J. Solid State Chem.*, 2013, **199**, 253–257.

[71] R. Lelieveld and D. J. W. IJdo, *Acta Crystallogr. B*, 1980, **36**, 2223–2226.

[72] K. J. Range, A. Gietl and U. Klement, *Z. Kristallogr. – Cryst. Mater.*, 1993, **207**, 147–148.

[73] H. Noel, J. Padiou and J. Prigent, *C. R. Acad. Sc. Paris C*, Jan 1975, **280**, 123–126.

[74] G. B. Jin, E. S. Choi and T. E. Albrecht-Schmitt, *J. Solid State Chem.*, 2009, **182**, 1075–1081.

[75] M. D. Ward and J. A. Ibers, *Acta Crystallogr. E*, 2014, **70**, i4.

[76] A. Daoudi and H. Noel, *Inorg. Chim. Acta*, 1987, **140**, 93–95.

[77] N. Rodier and P. Laruelle, *C. R. Acad. Sc. Paris C*, June 1970, **270**, 2127–2130.

[78] C. M. Kareis, S. H. Lapidus, J. H. Her, P. W. Stephens and J. S. Miller, *J. Am. Chem. Soc.*, 2012, **134**, 2246–2254.

[79] J. H. Her, P. W. Stephens, C. M. Kareis, J. G. Moore, K. S. Min, J. W. Park, G. Bali, B. S. Kennon and J. S. Miller, *Inorg. Chem.*, 2010, **49**, 1524–1534.

[80] K. T. Møller, M. B. Ley, P. Schouwink, R. Černý and T. R. Jensen, *Dalton Trans.*, 2016, **45**, 831–840.

[81] P. Schouwink, F. Morelle, Y. Sadikin, Y. Filinchuk and R. Černý, *Energies*, 2015, **8**, 8286–8299.

[82] L. Ye, Z.-X. Gong, C. Shi, J.-J. Ma, H. Liang, F.-W. Qi, D.-Y. E, C.-F. Wang, Y. Zhang and H.-Y. Ye, *CrystEngComm*, 2019, **21**, 7043–7047.

[83] Y.-L. Sun, X.-B. Han and W. Zhang, *Chem. Eur. J.*, 2017, **23**, 11126–11132.

[84] L. C. Gomez-Aguirre, B. Pato-Doldan, A. Stroppa, S. Yanez-Vilar, L. Bayarjargal, B. Winkler, S. Castro-Garcia, J. Mira, M. Sanchez-Andujar and M. A. Senaris-Rodriguez, *Inorg. Chem.*, 2015, **54**, 2109–2116.

[85] Z. Duan, Z. Wang and S. Gao, *Dalton Trans.*, 2011, **40**, 4465–4473.

[86] L. C. Gomez-Aguirre, B. Pato-Doldan, J. Mira, S. Castro-Garcia, M. A. Senaris-Rodriguez, M. Sanchez-Andujar, J. Singleton and V. S. Zapf, *J. Am. Chem. Soc.*, 2016, **138**, 1122–1125.

[87] Z. Wang, B. Zhang, T. Otsuka, K. Inoue, H. Kobayashi and M. Kurmoo, *Dalton Trans.*, 2004, 2209–2216.

[88] S. Chen, R. Shang, K.-L. Hu, Z.-M. Wang and S. Gao, *Inorg. Chem. Front.*, 2014, **1**, 83–98.

[89] I. E. Collings, J. A. Hill, A. B. Cairns, R. I. Cooper, A. L. Thompson, J. E. Parker, C. C. Tang and A. L. Goodwin, *Dalton Trans.*, 2016, **45**, 4169–4178.

[90] M. Maczka, A. Ciupa, A. Gagor, A. Sieradzki, A. Pikul, B. Macalik and M. Drozd, *Inorg. Chem.*, 2014, **53**, 5260–5268.

[91] B. Zhou, Y. Imai, A. Kobayashi, Z. M. Wang and H. Kobayashi, *Angew. Chem. Int. Ed.*, 2011, **50**, 11441–11445.

[92] R. Shang, G. C. Xu, Z. M. Wang and S. Gao, *Chem. Eur. J.*, 2014, **20**, 1146–1158.

[93] R. Shang, S. Chen, B. W. Wang, Z. M. Wang and S. Gao, *Angew. Chem. Int. Ed.*, 2016, **55**, 2097–2100.

[94] B. Q. Wang, H. B. Yan, Z. Q. Huang and Z. Zhang, *Acta Crystallogr. C*, 2013, **69**, 616–619.

[95] M. Maczka, J. Janczak, M. Trzebiatowska, A. Sieradzki, S. Pawlus and A. Pikul, *Dalton Trans.*, 2017, **46**, 8476–8485.

[96] J. A. Zienkiewicz, D. A. Kowalska, K. Fedoruk, M. Stefanski, A. Pikul and M. Ptak, *J. Mater. Chem. C*, 2021, **9**, 6841–6851.

[97] X. H. Zhao, X. C. Huang, S. L. Zhang, D. Shao, H. Y. Wei and X. Y. Wang, *J. Am. Chem. Soc.*, 2013, **135**, 16006–16009.

[98] Z. Y. Du, Y. Z. Sun, S. L. Chen, B. Huang, Y. J. Su, T. T. Xu, W. X. Zhang and X. M. Chen, *Chem. Commun.*, 2015, **51**, 15641–15644.

[99] Z. Y. Du, Y. P. Zhao, W. X. Zhang, H. L. Zhou, C. T. He, W. Xue, B. Y. Wang and X. M. Chen, *Chem. Commun.*, 2014, **50**, 1989–1991.

[100] J. Yang, Y. Huang, T. Fang, K. Qian, W.-B. Chen, X.-F. Yu, Y.-C. Ai, J.-L. Ye and X.-Y. Li, *Z. Naturforsch. B*, 2019, **74**, 335–339.

[101] K. Qian, Y. Xu, Z. Wang and J. Yang, *Z. Naturforsch. B*, 2017, **72**, 409–413.

[102] Y. Wu, S. Shaker, F. Brivio, R. Murugavel, P. D. Bristowe and A. K. Cheetham, *J. Am. Chem. Soc.*, 2017, **139**, 16999–17002.

[103] M. Maczka, A. Gagor, A. Pikul and D. Stefanska, *RSC Adv.*, 2020, **10**, 19020–19026.

[104] Y. Wu, T. Binford, J. A. Hill, S. Shaker, J. Wang and A. K. Cheetham, *Chem. Commun.*, 2018, **54**, 3751–3754.

[105] M. Maczka, A. Gagor, J. K. Zareba, D. Stefanska, M. Drozd, S. Balciunas, M. Šimėnas, J. Banys and A. Sieradzki, *Chem. Mater.*, 2020, **32**, 4072–4082.

[106] Q. Pan, Z. B. Liu, Y. Y. Tang, P. F. Li, R. W. Ma, R. Y. Wei, Y. Zhang, Y. M. You, H. Y. Ye and R. G. Xiong, *J. Am. Chem. Soc.*, 2017, **139**, 3954–3957.

[107] X. G. Chen, J. X. Gao, X. N. Hua and W. Q. Liao, *Acta Crystallogr. C*, 2018, **74**, 728–733.

[108] L. A. Paton and W. T. Harrison, *Angew. Chem. Int. Ed.*, 2010, **49**, 7684–7687.

[109] W.-Y. Zhang, Y.-Y. Tang, P.-F. Li, P.-P. Shi, W.-Q. Liao, D.-W. Fu, H.-Y. Ye, Y. Zhang and R.-G. Xiong, *J. Am. Chem. Soc.*, 2017, **139**, 10897–10902.

[110] G. Thiele and D. Messer, *Z. anorg. allg. Chem.*, 1980, **464**, 255–267.

[111] D.-X. Liu, K.-P. Xie, W.-X. Zhang, M.-H. Zeng and X.-M. Chen, *CrystEngComm*, 2021, **23**, 2208–2214.

[112] H. Y. Ye, Y. Y. Tang, P. F. Li, W. Q. Liao, J. X. Gao, X. N. Hua, H. Cai, P. P. Shi, Y. M. You and R. G. Xiong, *Science*, 2018, **361**, 151–155.

[113] Y.-L. Sun, C. Shi and W. Zhang, *Dalton Trans.*, 2017, **46**, 16774–16778.

[114] Y. L. Sun, X. B. Han and W. Zhang, *Chem. Eur. J.*, 2017, **23**, 11126–11132.

[115] S.-L. Chen, Z.-R. Yang, B.-J. Wang, Y. Shang, L.-Y. Sun, C.-T. He, H.-L. Zhou, W.-X. Zhang and X.-M. Chen, *Sci. China Mater.*, 2018, **61**, 1123–1128.

[116] S.-L. Chen, Y. Shang, C.-T. He, L.-Y. Sun, Z.-M. Ye, W.-X. Zhang and X.-M. Chen, *CrystEngComm*, 2018, **20**, 7458–7463.

[117] M.-L. Tong, J. Ru, Y.-M. Wu, X.-M. Chen, H.-C. Chang, K. Mochizuki and S. Kitagawa, *New J. Chem.*, 2003, **27**, 779–782.

[118] L. Zhou, X. Zheng, P. P. Shi, Z. Zafar, H. Y. Ye, D. W. Fu and Q. Ye, *Inorg. Chem.*, 2017, **56**, 3238–3244.

[119] F.-J. Geng, L. Zhou, P.-P. Shi, X.-L. Wang, X. Zheng, Y. Zhang, D.-W. Fu and Q. Ye, *J. Mater. Chem. C*, 2017, **5**, 1529–1536.

[120] M. M. Zhao, L. Zhou, P. P. Shi, X. Zheng, X. G. Chen, J. X. Gao, L. He, Q. Ye, C. M. Liu and D. W. Fu, *Chem. Eur. J.*, 2019, **25**, 6447–6454.

[121] Q. Li, *Acta Crystallogr. C*, 2015, **71**, 65–68.

[122] J. A. Hill, A. L. Thompson and A. L. Goodwin, *J. Am. Chem. Soc.*, 2016, **138**, 5886–5896.

[123] J. Lefebvre, D. Chartrand and D. B. Leznoff, *Polyhedron*, 2007, **26**, 2189–2199.

[124] H. L. B. Boström, J. A. Hill and A. L. Goodwin, *Phys. Chem. Chem. Phys.*, 2016, **18**, 31881–31894.